Optics Letters

Frequency dependent harmonic powers in a modified uni-traveling carrier photodetector

Yue Hu,[1,*] Curtis R. Menyuk,[1] Meredith N. Hutchinson,[2] Vincent J. Urick,[2] and Keith J. Williams[2]

[1]University of Maryland, Baltimore County, 1000 Hilltop Circle, Baltimore, Maryland 21250, USA
[2]Naval Research Laboratory, Photonics Technology Branch, Washington, DC 20375, USA
*Corresponding author: yuehu1@umbc.edu

Received 6 December 2016; revised 31 January 2017; accepted 5 February 2017; posted 6 February 2017 (Doc. ID 282323); published 20 February 2017

We use a drift-diffusion model to study frequency dependent harmonic powers in a modified uni-traveling carrier (MUTC) phododetector. The model includes external loading, incomplete ionization, the Franz–Keldysh effect, and history-dependent impact ionization. In three-tone measurements, the bias voltage at which a null occurs (bias null) in the second-order intermodulation distortion (IMD2) is different for the sum frequency and difference frequency. We obtained agreement with the experimental results. The bias null that appears in the IMD2 is due to the Franz–Keldysh effect. The bias voltage at which the bias null is located depends on the electric field in the intrinsic region, and the difference in the location of the bias null for the sum frequency and difference frequency is due to the displacement current in the intrinsic region. When the frequency is large, the displacement current is large and has a large effect on the harmonic powers. We also found that the bias null depends on the recombination rate in the *p*-absorption region because the electric field decreases in the intrinsic region when the recombination rate in the *p*-region decreases.

OCIS codes: (040.5160) Photodetectors; (060.5625) Radio frequency photonics.

https://doi.org/10.1364/OL.42.000919

Asymmetries in the amplitudes of lower and upper intermodulation distortion (IMD) tones are often observed in microwave devices that are subjected to two-tone or three-tone tests. These asymmetries are also observed in the photodetector measurements [1,2]. In a three-tone measurement, where the modulation frequencies are F_1, F_2, and F_3, the IMD power that is associated with the frequency combination $F_1 + F_2$ is different from the one at $|F_1 - F_2|$. In particular, the bias voltage at which a null occurs (bias null) in the IMD is different. The frequency dependence of the IMD power could be due to a memory effect, i.e., a bandwidth-dependent nonlinear effect. There are several studies of the memory effect in a microwave amplifier [3,4], but the physical reason for the IMD power difference in a photodetector has been unclear. In this Letter, we will use the drift-diffusion model to determine the physical origin of the IMD power difference in an MUTC photodetector.

Figure 1 show the structure of the MUTC photodetector [5]. The main difference between this structure and a UTC photodetecter is that there is a cliff layer between the collection layer and the absorption layer. The cliff layer is moderately doped. Without the cliff layer, the electric field is present throughout the entire intrinsic region. With a cliff layer, the electric field is mostly present in the InGaAs intrinsic layer instead of the entire intrinsic region. The electric field in the InGaAs intrinsic layer increases due to the cliff layer, which reduces the space charge effect. Another difference is that there is a thin intrinsic layer of InGaAs, which is used to increase the responsivity. Layers of InGaAsP are placed between the InP and InGaAs layers to help electrons transfer easily from InGaAs to InP, due to a decrease in the gap between the conduction bands.

A three-tone setup [6] was used to measure the harmonic powers in the device. The device output power was measured as a function of reverse bias voltage from 0 to 10 V in 0.25 V increments. The frequencies are 4.9 GHz, 5.0 GHz, and 5.15 GHz. The average photocurrent is 20 mA. We show the experimental results in Fig. 2. We can separate the IMD2 (second-order IMD powers) into two groups. One group contains the sum frequency powers at $F_1 + F_2$, $F_1 + F_3$, and $F_2 + F_3$, and the other group contains the difference frequency powers at $|F_1 - F_2|$, $|F_1 - F_3|$, and $|F_2 - F_3|$. In each group, the IMD2 behavior is the same. So, we only show the IMD2 powers for one element of each group, $F_1 + F_2$ and $|F_1 - F_2|$. However, we observe a significant difference between the IMD2 powers for the sum frequency ($F_1 + F_2$) and the difference frequency ($|F_1 - F_2|$). A bias null appears in both IMD2 powers, but the bias voltage at which the null is located is different.

We use the drift-diffusion equations [7–10] to model the MUTC photodetector [5], which have been modified to include the following effects: (1) field-dependent mobilities and diffusion coefficients for both holes and electrons, (2) a history-dependent impact ionization, and (3) the Franz–Keldysh effect.

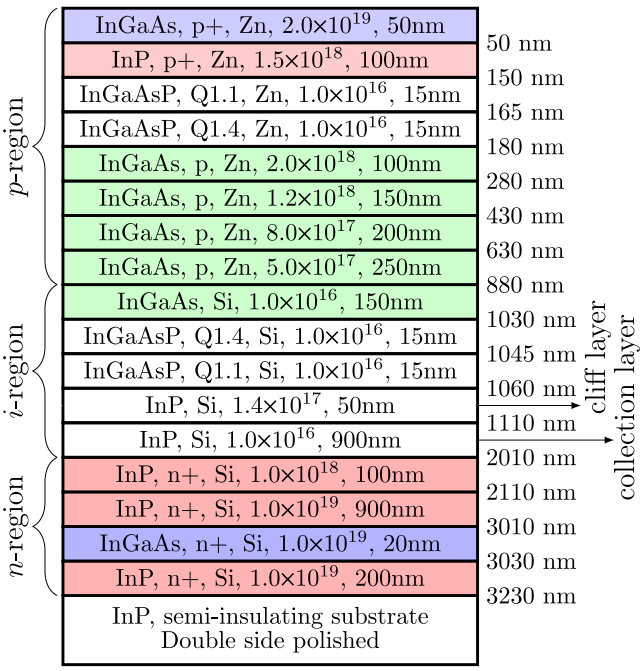

Fig. 1. Structure of the MUTC photodetector. Green indicates the absorption regions, which include an intrinsic region and a p-doped region. Red indicates highly doped InP layers; purple indicates highly doped InGaAs layers; and white indicate other layers.

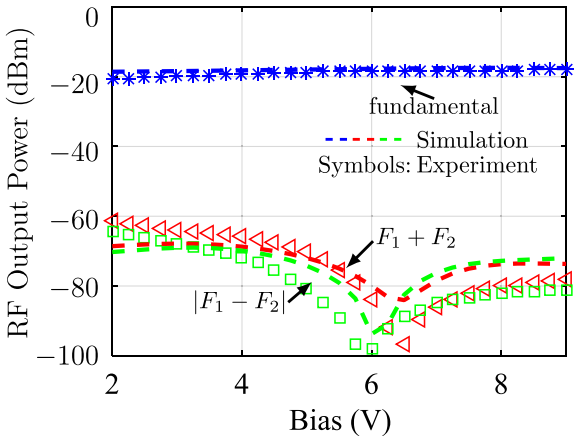

Fig. 2. Measured and calculated fundamental and IMD2 powers as a function of reverse bias for input frequencies $F_1 = 4.9$ GHz, $F_2 = 5.0$ GHz, and $F_3 = 5.15$ GHz.

The model consists of three equations that govern the dynamics of the electron density n, the hole density p, and the electric field $\mathbf{E}$ (negative gradient of the electrostatic potential, φ),

$$\frac{\partial(n - N_D^+)}{\partial t} = G_i + G_L - R(n,p) + \frac{\nabla \cdot \mathbf{J}_n}{q}, \tag{1a}$$

$$\frac{\partial(p - N_A^-)}{\partial t} = G_i + G_L - R(n,p) - \frac{\nabla \cdot \mathbf{J}_p}{q}, \tag{1b}$$

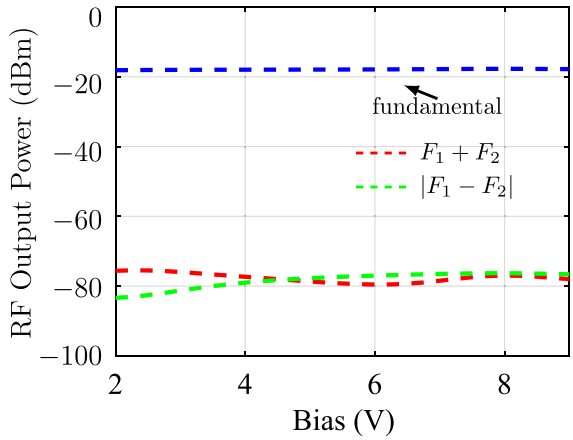

Fig. 3. Calculated fundamental and IMD2 powers as a function of reverse bias for input frequencies $F_1 = 4.9$ GHz, $F_2 = 5.0$ GHz, and $F_3 = 5.15$ GHz. The Franz–Keldysh effect is not included in the simulation.

$$\nabla \cdot \mathbf{E} = \frac{q}{\varepsilon}(N_D^+ + p - n - N_A^-), \tag{1c}$$

where q is the unit of charge (here positive), G_i and G_L are the impact ionization and photon generation rates, R is the recombination rate, ε is the permittivity of the semiconductor material, and N_D^+ and N_A^- are the ionized donor and acceptor impurity concentrations. The variables $\mathbf{J}_n$ and $\mathbf{J}_p$ are the current densities for electrons and holes. We use a three-tone setup, which is same as in the experiments. The generation rate may be expressed as

$$G_L = G_0\{1 + m_d[\sin(2\pi F_1 t) + \sin(2\pi F_2 t) + \sin(2\pi F_3 t)]\}, \tag{2}$$

where G_0 is the steady-state generation rate, m_d is the modulation depth, and F_1, F_2, and F_3 are the three-tone modulation frequencies.

We show the simulation results for the IMD2 power in Fig. 2, and the agreement with the experiments is good. We also obtain a bias null in the IMD2 power. The bias null in the difference frequency IMD2 power appears at around 6 V, while the bias null in the sum frequency IMD2 power appears at around 6.5 V, which agrees with the experiment.

Figure 3 shows the RF output power when the Franz–Keldysh effect is not included. We found that there is no bias null in the IMD2 power. As we discussed in [9], there are several sources of nonlinearity in high-current photodetectors. The combination of the load resistor and the Franz–Keldysh effect leads to the null in the harmonic power in this device. The absorption coefficient changes when the electric field changes in the device, so that the generation rate—especially in the intrinsic absorption region—changes as a function of the electric field. The nulls appear at biases where the change of absorption coefficient as a function of the electric field strength is small.

We have shown that the Franz–Keldysh effect is the reason for the null that appears in the IMD2 power, but we have not explained why the null position is different for the sum frequency and the difference frequency IMD2 powers. We note

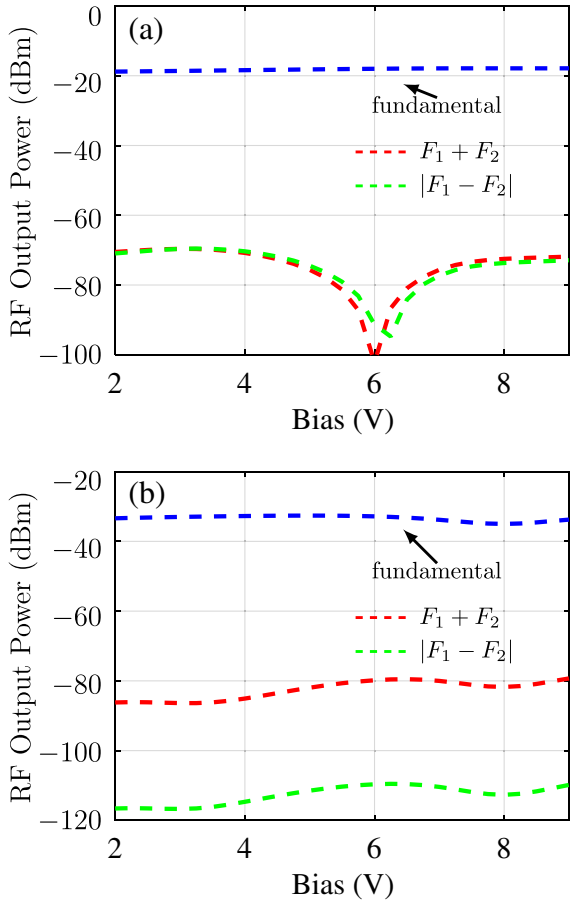

Fig. 4. Calculated fundamental and IMD2 powers as a function of reverse bias for input frequencies $F_1 = 4.9$ GHz, $F_2 = 5.0$ GHz, and $F_3 = 5.15$ GHz. (a) Displacement current is not included in the total current. (b) IMD2 power of the displacement current.

that the difference frequency of $|F_1 - F_2|$ is 100 MHz, and the sum frequency $F_1 + F_2$ is 9.9 GHz.

The current in the intrinsic region includes the electron current, the hole current, and the displacement current. In Fig. 4(a), we show the RF output current in the intrinsic region without the displacement current. We find that the bias nulls are the same for different modulation frequencies. The displacement current is responsible for the difference in the location of the rate change of the bias null for the sum and difference frequencies IMD2 powers. The displacement current depends on the rate at which the electric field in the intrinsic region changes. When the modulation frequency is large, the change of electric field increases, and the displacement becomes large and has a large effect on the harmonic powers. Figure 4(b) shows the IMD2 power of the displacement current. At the sum frequency $F_1 + F_2$, the IMD2 power of the displacement current is around −85 dBm, which is close to the IMD2 power of the total current. By contrast, the IMD2 power of the displacement current at the difference frequency $|F_1 - F_2|$ is about −125 dBm, which is much smaller than the IMD2 power of the total current. So, the displacement current does not affect the IMD2 power of the difference frequency.

From a circuit perspective, the displacement current is due to device capacitance. The impedance difference for different

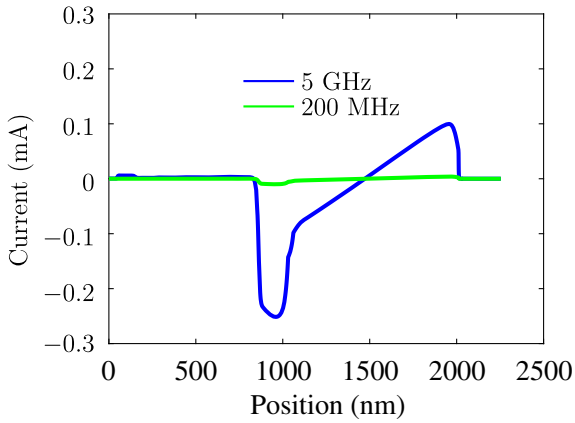

Fig. 5. Amplitude of the sinusoidally varying displacement current in the device at 200 MHz and 5 GHz.

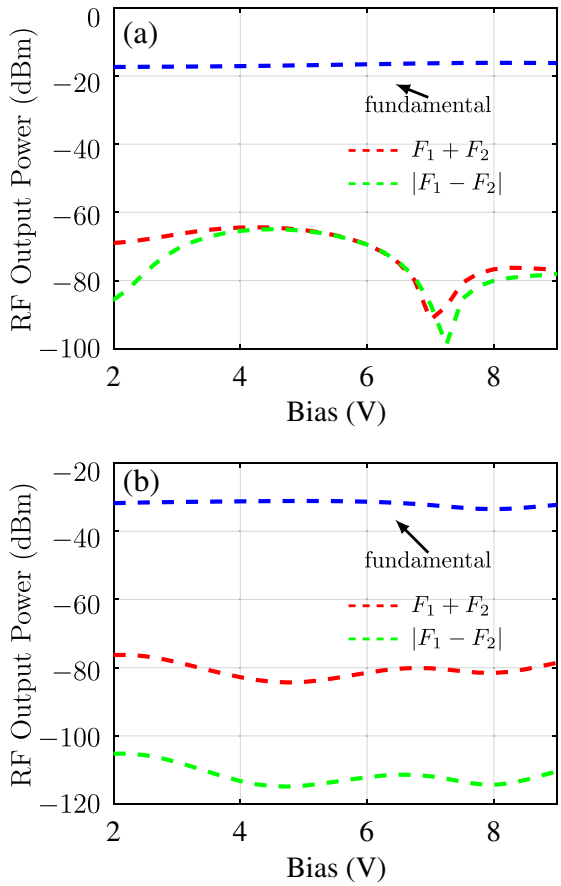

Fig. 6. Calculated fundamental and IMD2 powers as a function of reverse bias for input frequencies $F_1 = 4.9$ GHz, $F_2 = 5.0$ GHz, and $F_3 = 5.15$ GHz. The lifetime in the p-region is 5×10^{-11} s. (a) IMD2 power of the total current. (b) IMD2 power of the displacement current.

modulation frequencies leads to different displacement currents, which affect the location of the bias null in the IMD2 power. Figure 5 shows the largest displacement current when modulation is applied to the device for modulation

frequencies of 200 MHz and 5 GHz. We observe that the displacement current with a 5 GHz modulation is much larger than with a 200 MHz modulation. The displacement current is larger in the intrinsic absorption region, where the electric field is larger than it is in other regions.

Figure 6 shows the three-tone RF output powers as a function of applied bias, when the lifetime increases from 1×10^{-11} s to 5×10^{-11} s in the *p*-region. The photogeneration rate is the same as in Fig. 2. We find that the location of the bias null in the second-order harmonic powers are almost the same for the sum frequency and the difference frequency. The recombination rate in the *p*-region has a significant effect on the location of the bias null of the IMD2 power. When the recombination time increases, the recombination rate decreases in the *p*-region, so that more electrons enter the intrinsic region, increasing the electron density and decreasing the electric field in the intrinsic region. So, when the electric field decreases due to the increase in the electron lifetime in the *p*-region, the bias null moves to a larger voltage bias.

We also find that the electron diffusion coefficient is a factor in determining the position of the nulls. The direction of the electron diffusion is from the intrinsic region to the *p*-region. When the diffusion coefficient of the electrons in the *p*-region increases, more electrons diffuse into the *p*-region, so that the electron density decreases and the electric field increases in the intrinsic region. The increase in the electric field leads to a longer depletion region, and the capacitance increases. The increased capacitance leads in turn to smaller impedances for higher modulation frequencies.

In conclusion, we obtained agreement with experiments for the location of the bias nulls in the IMD2 power for different modulation frequencies. We investigated the physical origin of the nulls in the IMD2 power and we found that the Franz–Keldysh effect causes the bias nulls. The difference in the location of the bias nulls between the sum frequency and difference frequency IMD2 powers is due to the displacement current in the intrinsic region. When the frequency is high, the displacement current is large and affects the harmonic powers. We also found that the recombination rate in the *p*-region affects the bias null in the IMD2 power. When the recombination rate decreases, more electrons enter into the intrinsic region, which decreases the electric field in this region. Then the bias null moves to a higher bias. The diffusion coeffient in the *p*-region is also a factor in determining the location of the bias null.

Funding. U.S. Naval Research Laboratory (NRL) (N00173-15-1-G905).

REFERENCES

1. M. N. Hutchinson, S. Estrella, and M. Mashanovitch, in *IEEE Avionics and Vehicle Fiber-Optics and Photonics Conference (AVFOP)* (2016), paper WA2.2.
2. N. J. Frigo, M. N. Hutchinson, and J. R. Peasant, J. Lightwave Technol. **34**, 4696 (2016).
3. N. B. D. Carvalho and J. C. Pedro, IEEE Trans. Microw. Theory Tech. **47**, 2364 (1999).
4. N. B. D. Carvalho and J. C. Pedro, IEEE Trans. Microw. Theory Tech. **50**, 2090 (2002).
5. Z. Li, H. Pan, H. Chen, A. Beling, and J. C. Campbell, IEEE J. Quantum Electron. **46**, 626 (2010).
6. M. N. Draa, A. S. Hastings, and K. J. Williams, Opt. Express **19**, 12635 (2011).
7. Y. Fu, H. Pan, Z. Li, A. Beling, and J. C. Campbell, IEEE J. Quantum Electron. **47**, 1312 (2011).
8. Y. Hu, B. S. Marks, C. R. Menyuk, V. J. Urick, and K. J. Williams, J. Lightwave Technol. **32**, 3710 (2014).
9. Y. Hu, T. F. Carruthers, C. R. Menyuk, M. N. Hutchinson, V. J. Urick, and K. J. Williams, Opt. Express **23**, 20402 (2015).
10. Y. Hu and C. R. Menyuk, *International Topical Meeting on Microwave Photonics (MWP)* (2013), pp. 282–285.